

PIGMENT COATING PERMEABILITY: measurement and correlation with wetting front penetration

J. Schoelkopf¹
Senior Scientist

P.A.C. Gane
Vice President Research & Development
Paper & Pigment Systems

C.J. Ridgway
Senior Scientist

Omya AG
CH 4665 Oftringen
Switzerland

ABSTRACT

While porosity may be the most important geometrical description of a porous structure, permeability is probably the most important structural characteristic. In paper science air permeation is the most widely used technique to determine permeability and this is used mainly with uncoated papers. The focus of the work here is on the permeability of pigmented coatings alone and not as paper samples. The permeabilities of a range of porous samples are measured using a specially-constructed high pressure liquid permeation cell. Data of this kind have not been reported before in the literature. The samples consist of compacted fine isotropic mineral pigment - calcium carbonate - compressed over a range of compaction pressures resulting in a range of porosities. These samples have pore-throat diameters typically finer than 0.1 μm . The porosities and the pore size distributions of the samples have been determined by means of mercury porosimetry. The permeability is seen under certain conditions not to obey the well-known linearity of the Darcy relation as a function of applied liquid pressure differential. A considerable pressure-flux hysteresis is observed following saturation by imbibition. Furthermore, it is seen that there is no direct linear correlation between permeability and porosity, despite the use of a constant pigment particle size distribution and, hence, skeletal size distribution. The measured permeability displays a local maximum at a fractional porosity of approximately 0.26 with a further distinct drop at around 0.27. Interestingly, this phenomenon is seen to correlate with data from water droplet equilibrium distribution within the same structures.

Taking into account the effects of earlier-proposed mechanisms of preferred pathway flow and film flow during imbibition, it is postulated that some pores remain unfilled during imbibition prior to the permeability study, such that there remains entrapped air or vapour phase in microscopic ganglia. This air does not dissolve in the aliphatic mineral oil used in the experiments. Structures with a delineated pore-throat structure will probably lead generally to observed non-linear phenomena within the range of dimensions studied here, which can have implications, amongst others, for microscopic filtration, catalysis and absorption phenomena.

Keywords: imbibition into coating structures, permeability of coatings, preferred pathway flow, permeability hysteresis, liquid-coating interactions.

INTRODUCTION

Earlier studies [1] showed that the depth of liquid penetration into a pigmented network exceeded the equivalent saturated pore volume of the sample behind the wetting front. This finding indicated that a substantial portion of a pigmented coating structure remains unfilled as the fluid phase of an ink is absorbed. The amount of unfilled pores existing during the dynamic absorption of a liquid was also shown to be dependent on the network porosity, a local maximum in penetration depth was seen to occur for coating porosities in the range of ~ 0.26 -

¹ Author to whom correspondence should be addressed

0.27. Subsequent modelling of the absorption of liquid into a model network structure (Pore-Cor²), based on a Bosanquet wetting algorithm, showed that this excluded pore volume could be accounted for by considering the differential inertial retardation between liquid entering large and small pores of low aspect ratio; the finer pore structure wetting preferentially compared to the larger cross-section pores [2].

The adoption of an inertial wetting regime leads to an observed irregularity in the wetting front [3] and so to a definition of a preferred pathway of wetting in an interconnected network of pores. Following the work of Sorbie *et al.* [4] on a pore doublet, Ridgway *et al.* [5] extended the analogy to a complete network model, showing that pores of certain aspect ratio (length/diameter) imbibe preferentially. This aspect ratio, for typical structures of similar porosity to those found in paper coatings, approximated to 0.5. The wetting front, therefore, proceeds fastest in those finer pores having dimensions where the length of the feature is approximately half of its diameter. This is particularly relevant for structures composed of blocky pigment morphologies, such as fine ground calcium carbonate and some secondary low aspect ratio fine US clays, and explains the rapid ink tackification behaviour on glossy coatings made from these pigment types.

The volume uptake of liquid into porous pigmented media has also been reported [6] and, for structures similar to paper coatings, was shown to follow a \sqrt{t} relationship, where t is the time taken to absorb a given volume. This, however, cannot be interpreted as following a Lucas-Washburn dynamic as the uneven wetting front prevents a unique definition of an equivalent hydraulic radius for the assumed values of surface energy and liquid viscosity [3]. Until now, it has been impossible to define the long time physical resistance force involved in limiting the liquid flow as all inertial wetting equations only apply a viscous resistance within those pores actually being filled under the given conditions of the equation, i.e. resistance in the pores only at the wetting front itself. This also explains why modelling the volume absorption using inertial wetting algorithms only works at short times [2], i.e. the resistance force is over-estimated by a simple mass balance approach applied only to those pores involved in the wetting algorithm.

THEORY

We briefly look at permeation, which is the motion of a liquid flowing through a porous substrate without a specification of an internal driving force. It is mostly defined for an external pressure-driven process in an effectively saturated sample. Hilfer [7] states that the permeability is the most important physical property of a porous medium in much the same way as porosity is its most important geometrical property. The permeability K is expressed using Darcy's Law [8], equation (1),

$$q = \frac{r^2 A \Delta P}{8 \mathbf{h} l} = K \frac{A \Delta P}{\mathbf{h} l} \quad (1)$$

balancing the driving pressure ΔP with the viscous drag derived from the Poiseuille equation, equation (2)

$$q = \frac{\delta r^4 \Delta P}{8 \mathbf{h} l} \quad (2)$$

where q is the volumetric flow rate, r is the radius of the circular tube assumed in the Poiseuille analysis representing the equivalent flow dimension of a unit cross-sectional area of the sample, \mathbf{h} is the fluid viscosity, A the total sample cross-sectional area and l its length. Darcy pioneered the topic of permeability, formulating the classical relationship given in equation (1). This equation has been widely adopted, has been adapted to more complex situations and has also been related to further structural parameters. Among the more popular extensions is the Carman-Kozeny approach [9], often called the "hydraulic radius theory", linking the void volume in a porous medium, \mathbf{f} with its inner specific surface area, s ,

$$r_h = \frac{\mathbf{f}}{s(1-\mathbf{f})} \quad (3)$$

² Pore-Cor is a software package developed by the Environmental and Fluid modelling Group, University of Plymouth, Devon, PL4 8AA, U.K.

where r_h is the hydraulic radius, and

$$K = \mathbf{x} \frac{\mathbf{r}g}{\mathbf{h}} \frac{\mathbf{f}}{\mathbf{t}^2 (1 - \mathbf{f})^2 s^2} \quad (4)$$

where \hat{t} is a function of the tube cross-sectional shape, (for cylinders $\hat{t} = 0.5$), \mathbf{r} is the density of the fluid, g is the acceleration due to gravity, assumed acting for vertical flow, and δ stands for a tortuosity term

$$\mathbf{t} = l_e / l \quad (5)$$

where l_e represents the effective path length through a sample. For details and variations, the reviews of van Brakel [10] and Dullien [11] give further insight.

In soil and petroleum science, K is often employed in the form of a permeability tensor to describe the permeation characteristics in a spatial (mostly macroscopic) context. Relative permeability describes permeation as a function of saturation with a third phase.

Pigment-related work concerning the permeability of a growing filtercake of paper coating particles was recently reported by Lohmander *et al* [12]. Much similar work has been carried out considering fibres, as the permeability response of a forming fibre mat is naturally the basis of paper making.

The limits of the Darcy regime have also been analysed. They can be exceeded by the presence of turbulent flow, liquid circulating in pores (pore-level eddies), entrapped ganglia of a different phase in small capillary features, which may start to move at a pressure threshold value (breakthrough phenomena) and at very low flow rates where interactions between the fluid and the pore walls become important, [7,13,14,15].

EXPERIMENTAL METHOD AND MATERIALS

A method was developed in which consolidated pigment structures are formed without a binder [1]. We concentrate here on the use of natural calcium carbonate derived from Orgon limestone, wet ground in the presence of polyacrylate and subsequently spray dried with a particle size distribution of 91 wt% < 5 μm , 55 wt% < 2 μm and 30 wt% < 1 μm , as commercially available as Hydrocarb 60 OG from Omya.

By applying different consolidation pressures, a wide range of usable porosities can be obtained which lend themselves to being well characterised using mercury porosimetry. The key point is that without change of the surface chemistry or intrinsic skeletal geometry a range of usable porosities and d_{50} pore diameters can be achieved (d_{50} is the Laplace diameter at 50 % intrusion volume of the mercury intrusion curve). The compressed tablet structures are ground into samples of cuboid shape, [2], and are embedded in epoxy resin as described previously, [16].

Porosimetry parameters of the experimental sample structures used in this study are given in Table 1 The properties of the used mineral oil "PKWF 6/9 af neu" from Haltermann are shown in Table 2.

ϵ_g	d_{50}
/%	/ μm
23.02	0.091
24.63	0.098
26.34	0.109
26.73	0.118
26.98	0.115
27.04	0.115
32.98	0.164
33.07	0.164

Table 1 The porosities and pore sizes of the structures used for permeability experimentation with oils.

	Viscosity	Surface tension	Density	Boiling point
	/ Pa s $\times 10^{-3}$	/ Nm ⁻¹ $\times 10^{-3}$	/ kgm ⁻³	/ °C
PKWF 6/9 af neu	4.3	27.4	805	160 - 290

Table 2 Overview of the liquid properties

Calculation of required pressures

To use this work for comparisons in the wider context of the impact of permeability on the absorption dynamic [16], the measurement of the absolute liquid permeability must be made using a differential pressure which is (i) of a magnitude which moves the fluid through the structure at a rate regime similar to that experienced during imbibition [17], while (ii) generating a flow regime which is laminar rather than turbulent, so that Darcy's law is valid. Condition (ii) may follow naturally from condition (i), however calculations were carried out for both conditions to check that the flow is in the correct regime. Details are given in the literature [18].

Permeation apparatus

The cell designed used for the pressurised permeability experiments is shown in Fig. 1. The use of the resin to embed the cuboid porous pigment samples (see below) allows for rigid clamping and sealing of the sample into the pressure cell chamber. A micro-balance records the amount of permeated liquid as a function of time and data is sampled using a specially-developed software developed within Omya AG³. A comprehensive description of the apparatus and the method is given in [16].

³ Software can be obtained on request from Dr. D. Spielmann, Omya AG Postfach 32, CH 4665 Oftringen, Switzerland

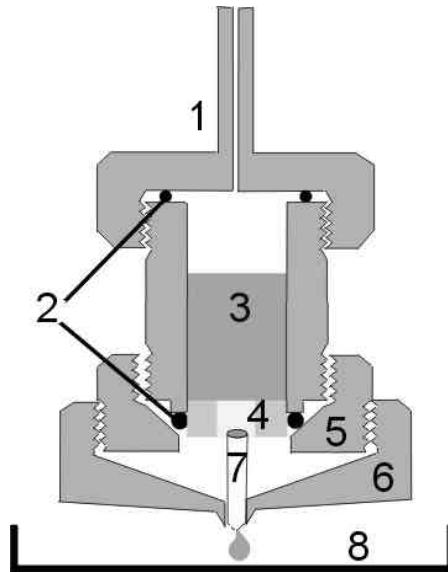


Fig. 1 Permeability measurement cell: 1) lid with pressure inlet, 2) sealing O-rings, 3) liquid in cell; outer diameter = 40 mm, 4) porous sample embedded in resin disc of diameter = 30 mm, 5) fixing ring compresses the o-ring which seals the resin disc, 6) security shroud and drop collector, 7) drop captor (Teflon tubelet), 8) dish on micro-balance.

RESULTS AND DISCUSSION

The first results showed an unexpected behaviour in that the flux at a constant pressure did not appear to be constant with time. An extreme example showed no flow at 3 bar differential pressure, but significant flow when the differential pressure was increased to 7 bar, which then continued proportionally reducing when the pressure was again lowered to 3 bar.

Examples of less extreme behaviour are shown in the graphs in Fig. 2.

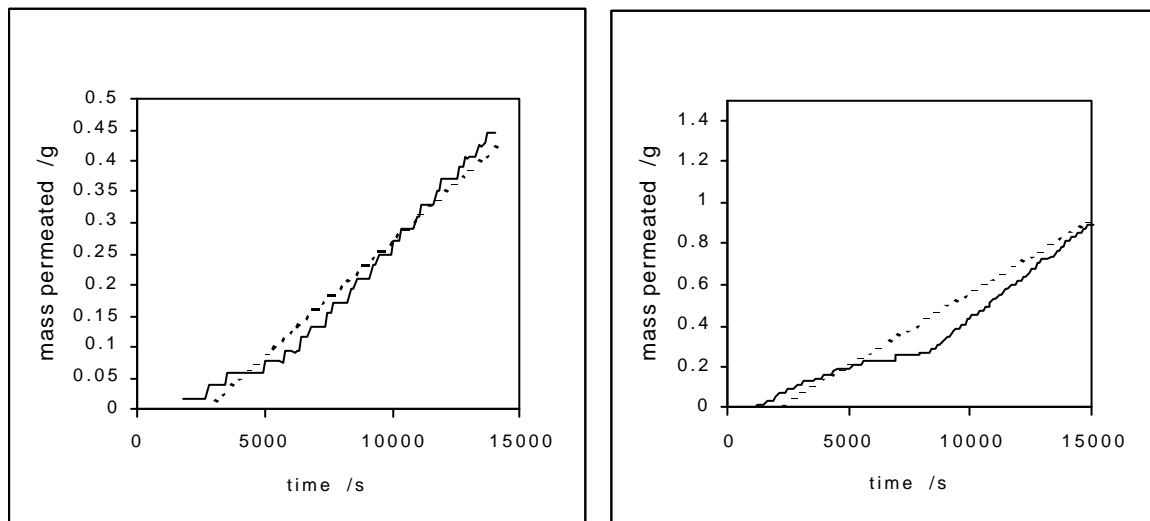


Fig. 2 Non-linear flow at constant pressure, left: 7.22 bar, 23.02 % porosity, right: 5.10 bar, 24.63 % porosity.

It was suspected that entrapped air bubbles could be the cause. If they start to move or become compressed, constant flow can only be achieved when the air is displaced or moved into stable trapping positions consistent

with the applied pressure and resulting flow. In order to investigate this issue further a hysteresis experiment was performed.

The sample was handled with the utmost care, making sure that no air could be introduced and trapped during the sample saturation or during the mounting into the measurement cell. A pressure hysteresis loop was then recorded as shown in Fig. 3.

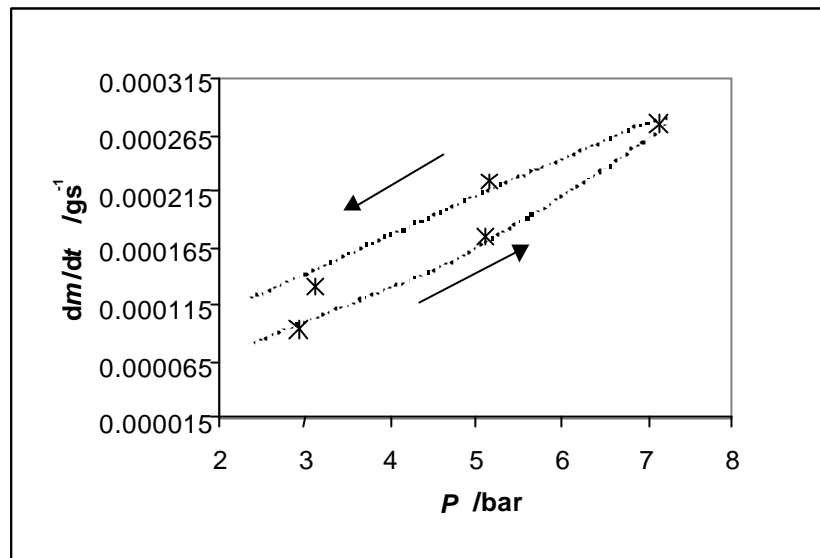


Fig. 3 Hysteresis of flow as a function of pressure: fractional porosity = 0.3298.

Clearly, the dependence of flow on sample pressure history (applied differential pressure) is evident. Once again, the flux is dependent on the starting pressure. If the effect would be due to pore-scale eddies or similar phenomena, hysteresis would not necessarily be expected. So, the previous assumption of trapped air bubbles, which at a given pressure threshold value may start to move and are partly extruded, seems to be the most likely answer. The measurement routine above, starting with the highest pressure first, ensured, at least, that there was no further bubble motion at lower pressures, but the amount of remaining entrapped air is not yet known. It has to be further assumed that due to the extreme care taken, the entrapped vapour bubbles do not occur during the sample handling after the supersource soaking but during the supersource imbibition itself.

Cycles of measurements were thus performed, first with the highest possible pressure (≈ 7 bar) and then recorded in descending order of pressure. A decreasing series of pressure steps are used to record the permeation flow over a reasonable amount of time to achieve a plot with a usable gradient. Such an experimental data set is shown in Fig. 4. Each step in the recorded curve is caused by one drop falling into the weighing pan. By making a linear regression analysis using Microsoft Excel, a gradient is determined which represents a flow rate of mass per unit time. It is clearly visible that the flow is in the necessary steady state at a constant pressure.

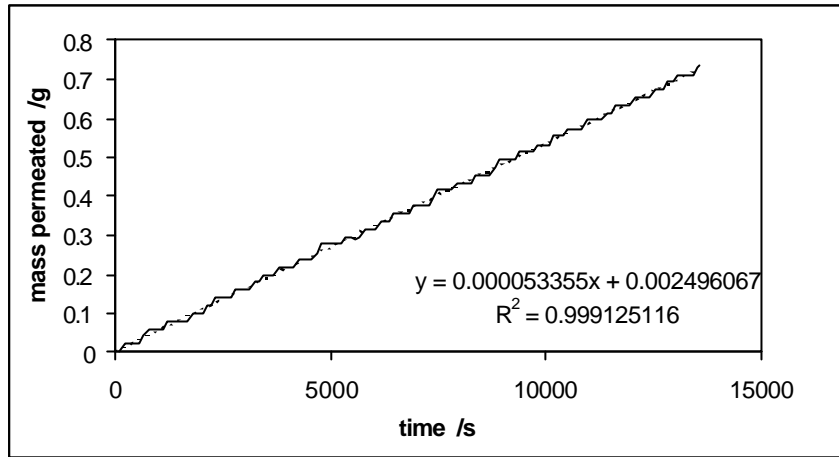


Fig. 4 Typical permeation curve, porosity =26.34 %, $P=4.82$ bar.

Determining gradients of further samples in this manner gave the data in Fig. 5. Although these plots look reasonable in terms of pressure / flow rate ratios and seem also to track with the porosities, they do not yet contain the sample size parameters needed to derive a permeability.

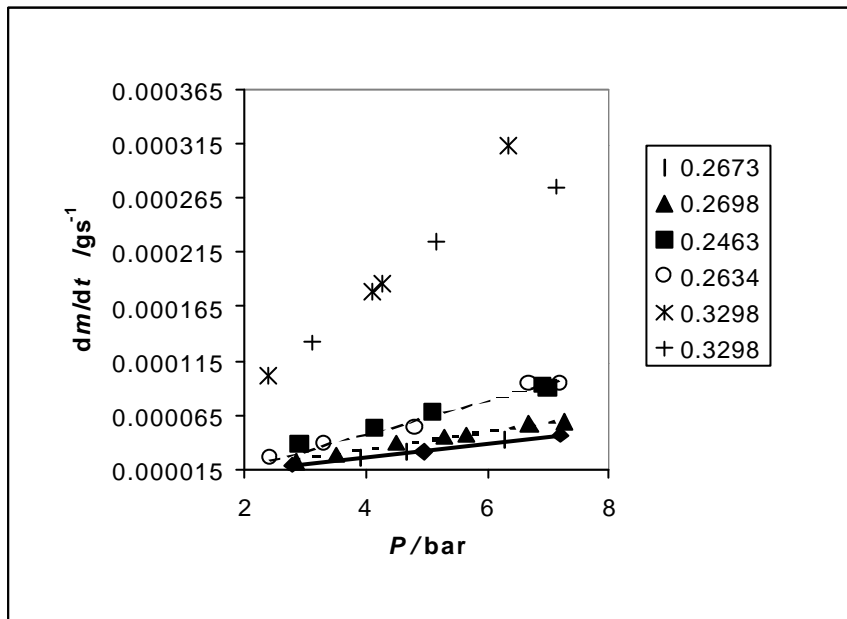


Fig. 5 Permeation gradients in a series of different porosity samples as a function of applied pressure (legend shows fractional porosities as measured by mercury porosimetry).

As soon as an "equivalent hydraulic capillary" radius $r_{ehcDarcy}$ is calculated by solving equation (1) where the term r is now $r_{ehcDarcy}$ and inputting the necessary dimensions of the sample, $r_{ehcDarcy}$ falls out of correlation with porosity, Fig. 6. The consequence is that porosity in these samples seems not to be the linear controlling factor of permeability.

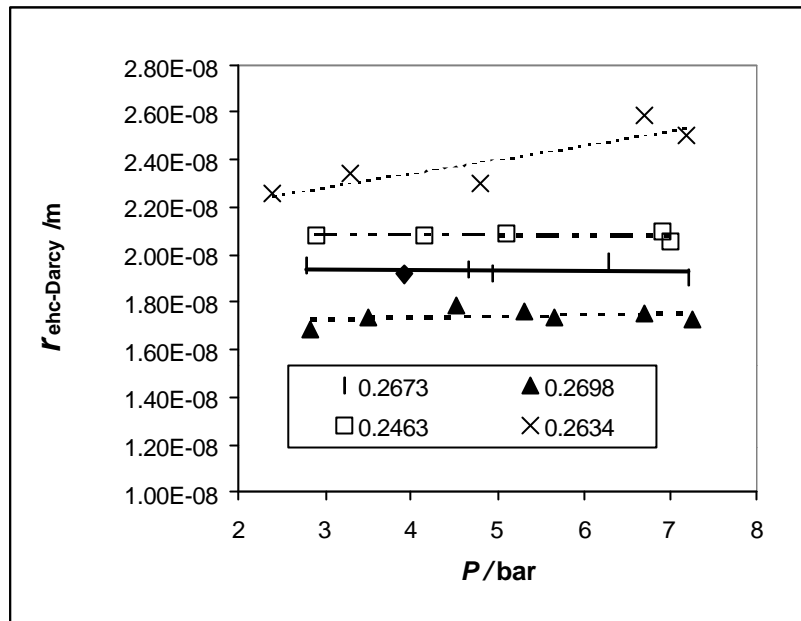


Fig. 6 Hydraulic radii not tracking with porosities (fractional porosities shown in legend).

This is an important finding in the science of paper coating structures as it is often *falsely* assumed that "openness" is implied by high porosity, which in turn means high absorption rate. In fact the contrary is often true with high driving forces for absorption of small liquid quantities being associated with low porosity fine pore networks. Similarly, high consumption of such liquids as lacquers and varnishes is in fact due to drainage effects which are in turn a function of permeability and not necessarily porosity.

Theory of entrapped bubbles

The finding that imbibition saturation leaves the sample with some entrapped air is in contrast to earlier statements, where it is described that a range of different liquids under supersource conditions imbibe into the whole pore structure present as determined by independent methods, i.e. by mercury porosimetry and Archimedes calculations [1]. How can these apparent contradictions be explained, and can they contribute to a better understanding of flow mechanisms during imbibition?

Assume the dimensions of one of the porous pigment samples has a cross-sectional area of 1 cm^2 and a volume of 1 cm^3 . It is known that the skeletal particles are in an average size range of $1 \mu\text{m}$. It follows that a row of 10 000 particles can line up along the sample edge, and in one in-planar layer of, say, cubic packing there are 10^8 particles. Assume there is 1 pore between 2 particles and omit the boundary zones in order to get a rough estimate of 99 960 000 pores per layer and therefore 9.99×10^{11} pores in the sample. Suppose a mean pore size is such that a spherical bubble fits into it with a diameter of $0.2 \mu\text{m}$. (This would be the case for particles with a radius of $1 \mu\text{m}$ in tetrahedral packing, [19,20], for finer particles the argument for this bubble size would be even stronger.) Such a bubble has a volume of $0.00418 \mu\text{m}^3$. So if one planar layer of pores is completely blocked by entrapped bubbles, the summation of the bubbles' volume is $418 432.56 \mu\text{m}^3$. This is equivalent to a mass of 0.3368 ng of displaced liquid as calculated using the mineral oil of $6/9$ ($\rho = 805 \text{ kgm}^{-3}$), which is far less than a microbalance can detect. Therefore, even with millions of entrapped bubbles in a sample they cannot be gravimetrically detected. So although the sample saturates as well as a sensitive balance can determine, there may well be a significant number of pores remaining that contain vapour. According to the size of an individual bubble, and the size and geometry of its host void, there are two distinct types of behaviour. The extreme behaviour mentioned above can be attributed to air bubbles which move and are flushed from the sample under pressure. The less extreme behaviour is due to air bubbles which move slightly or merely compress under increased pressure. The effect on permeability caused by both types of behaviour decreases with pressure, as compensated for in the experimental procedure.

The preferential wetting pathways during imbibition, as described in detail in previous work [2,5,21] are likely to cause the formation of the bubbles, since wetting through fast pathways overtakes that in slow pathways, and the exit route of air from the slow pathway is potentially cut off, thus producing a trapped bubble.

Linked to this potential effect is the evidence of adsorbed layers of water on the inner surface of the porous network and the known phenomenon of capillary condensation. This results in micro-pores filled by water which is also not soluble in the mineral oil and may block the relevant ganglia. As this effect is expected only in micro-pores it presumably does not influence the permeation behaviour significantly, which is determined mostly by pathways of interconnected large voids. This latter argumentation also allows us to surmise that the entrapped air is associated with the larger voids as it impacts strongly on the permeability which is mostly controlled in volume terms by the larger voids. This supports the proposition that the liquid during imbibition fills the finer pores first at the wetting front.

PERMEABILITY IN RELATION TO POROSITY

After one cycle of pressure increase and decrease, the hysteresis discussed above was overcome in all the samples tested. Accurate determination of permeability is possible using the post hysteresis cycle data, and Darcy permeability coefficients can be established.

Permeability was shown to be dependent on porosity but not monotonically, Fig. 7. A similar behaviour was previously seen from the penetration depth of fluid as applied from a droplet of known volume, Fig. 8, [1]. Fig. 7 shows that the permeation follows the same local maximum in relation to coating porosity (0.25 - 0.28) as was seen in the droplet penetration experiment as defined in terms of a pore filling level.

The level of pore filling in the droplet experiment is expressed as the difference ($V_{\text{simdyed}} - V_{\text{theodyed}}$), where V_{simdyed} represents the simulated geometrically approximated space reached by the dyed liquid using a model spheroid corresponding in shape and volume to the observed penetrated volume into the tablet. The theoretical penetration volume that would have occurred if all the void space was filled by the liquid is given by

$$V_{\text{theodyed}} = \frac{V_{\text{appliedink}}}{f_{\text{Hg}}} \quad (6)$$

where f_{Hg} is the porosity determined by mercury porosimetry. The difference ($V_{\text{simdyed}} - V_{\text{theodyed}}$) showed a marked transition as a function of the porosity. The limitation in the span of comparison was due to limited sample quantities for the droplet experiments, but the correspondence between permeability and the unfilled volume parameter is uncanny.

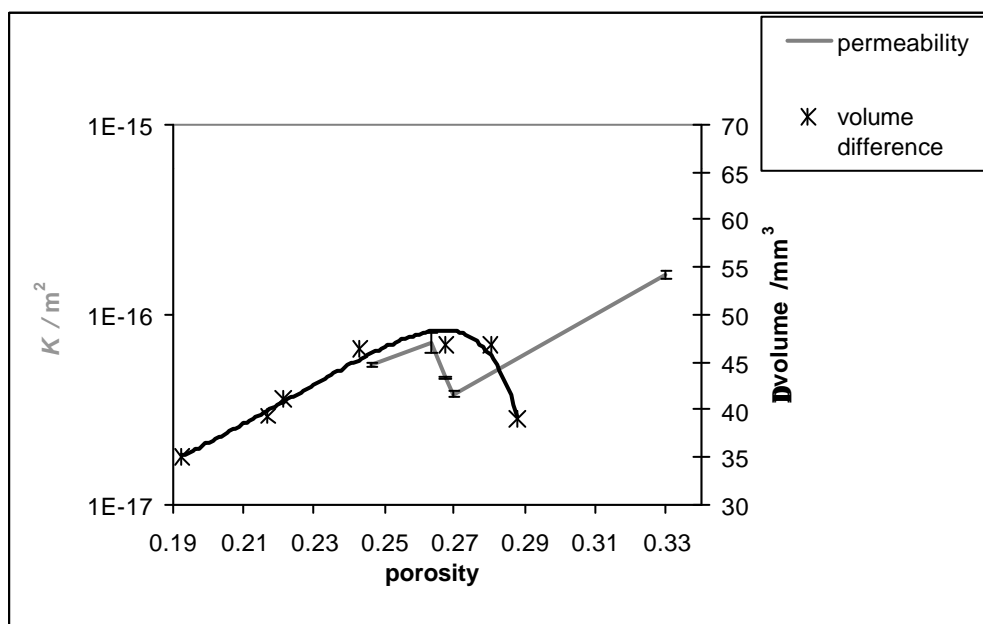


Fig. 7 Experimental permeability K compared to volume difference in pore filling (where volume difference = 0 would indicate completely filled pores)

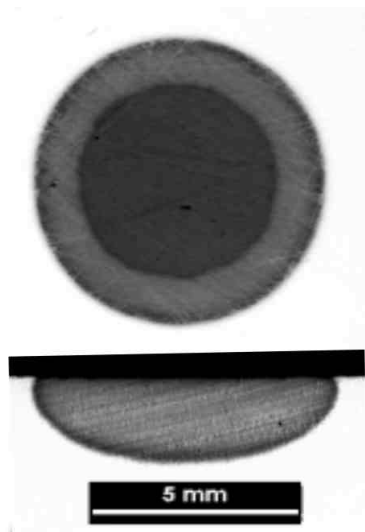


Fig. 8 An example of a droplet of imbibed dyed water into a pigment tablet, top: surface spread., below: cross-sectional cut showing liquid equilibrium distribution.

Remembering that the same pigment particle size was used throughout the experiments, the abrupt change in permeability as a function of porosity could in practice correlate in real paper samples with different levels of exposure to calendering, variations in shrinkage and differential surface compaction. All these factors mean that discrete transitions in permeability can be expected to occur in real systems exaggerating spatial effects such as mottle and absorbency in general. To explain this behaviour we postulate two possibilities:

- i) A combination of change of the throat sizes (crevices between particles at their mutual "closest" point) and connectivity. That this combination of parameters might be the cause could be explained by conformal changes in the compacting particles as mentioned by Toivakka and Nyfors [23], finding connectivities up to 9 for some packing modes.
- ii) Another explanation could be that under the inter-particle stresses during compaction agglomerates break up. In the agglomerated stage the interstitial voids are smaller than in the de-agglomerated stage. Both proposals would lead to temporarily larger voids in the structure, thus influencing permeability.

Permeability controls the penetration depth of a given volume of liquid, where that liquid volume is less than the total pore volume of the sample. This is confirmed since the permeability follows closely the local penetration depth maximum as a function of porosity. Permeability is therefore correct measure to use to determine the flow resistance behind the uneven wetting front within a network porous structure, and indicates that this corresponds with the absorption-saturated flow resistance.

Observations made using liquid permeability must be viewed with the boundary conditions of imbibition into a network structure of given pore size and shape being kept in mind. Experiments, for example, with uncoated paper samples as the embedded porous material showed no hysteresis, and therefore no apparent air entrapment during absorption [22].

CONCLUSIONS

An hysteresis in liquid permeability of porous pigmented coating structures was observed when performing an up-down sweep of driving pressure on an imbibition-saturated sample. Taking into account the effects of earlier discussed mechanisms of preferred pathway flow and film flow during imbibition, it is postulated that some pores remain unfilled such that there is entrapped air or vapour phase in some parts of the pore structure. This air may dissolve in polar liquids but does not dissolve in aliphatic mineral oil used in the experiments and typical of the diluent used in offset printing inks. The subsequent compression and/or expulsion of the air depending on pressure and flow leads to locally varying permeability to liquids.

The experimental permeability of pigmented structures once air is expelled or immobilised is seen not to be a monotonic function of porosity. With the coating pigment tested, it passes through a local maximum at a fractional porosity of 0.263 with a further decrease at a porosity of 0.27. This unexpected behaviour tracks well with observations previously made with droplet absorption experimentation where the level of mean liquid content in a porous medium at equilibrium goes through a minimum in the regime between porosities of 0.24 - 0.28. In this case, minimum mean liquid content in a porous medium parallels with maximum penetration depth of a given liquid volume. It is easy to understand how different areas of compactions of a coating will lead to different porosities and, from this work, a non-linear permeability response across these areas, in turn leading to an enhanced tendency for print mottle.

Combining these new data with previous findings [1,2,3,5,6,21,24] it is now possible to establish an improved model for liquid absorption into a network structure. The driving force is defined by the capillarity, the wetting front is defined by the inertial selectivity creating a selection mechanism defining the response to the capillarity, and the volume drag component under equilibrium absorption conditions is defined by the permeability of the structure. Prior to the establishment of the equilibrium absorption dynamic, the local preferred pathway features provide the specified resistance network for flow. This model explains the difference between short time absorption and longer time absorption during the setting of an ink on paper [25,26].

REFERENCES

1. Gane, P. A. C., Schoelkopf, J., Spielmann, D. C., Matthews, G. P., and Ridgway, C. J., "*Fluid transport into porous coating structures: some novel findings*", Tappi Journal, 83(5), 2000, p77-78
2. Schoelkopf, J., Ridgway, C. J., Gane, P. A. C., Matthews, G. P., and Spielmann, D. C., "*Measurement and Network Modeling of Liquid Permeation into Compacted Mineral Blocks*", Journal of Colloid and Interface Science, 227, 2000, p119-131
3. Schoelkopf, J., Gane, P. A. C., Ridgway, C. J., and Matthews, G. P., "*Practical observation of deviation from Lucas-Washburn scaling in porous media*", Colloids and Surfaces A: Physicochemical and Engineering Aspects, 206(1-3), 2002, p445-454
4. Sorbie, K. S., Wu, Y. Z., and McDougall, S. R., "*The extended washburn equation and its application to the oil/water pore doublet problem*", Journal of Colloid and Interface Science, (174), 1995, p289-301
5. Ridgway, C. J., Gane, P. A. C., and Schoelkopf, J., "*Effect of capillary element aspect ratio on the dynamic imbibition with porous networks*", Journal of Colloid and Interface Science, 252, 2002, p373-382
6. Schoelkopf, J., Gane, P. A. C., Ridgway, C. J., and Matthews, G. P., "*Influence of Inertia on Liquid Absorption into Paper Coating Structures*", Nordic Pulp and Paper Research Journal, 15(5), 2000, p422-430
7. Hilfer, R., "Transport and Relaxation Phenomena in Porous Media", John Wiley & Sons, Inc., New York, 1996
8. Darcy, H., Les Fontaines Publiques de la Ville de Dijon. Dalmont, Paris, 1856
9. Carman, P. C., "*Fluid Flow Through Granular Beds*", Transactions of Institution of Chemical Engineers (London), 15, 1937, p150-166
10. van Brakel, J., "*Pore Space Models for Transport Phenomena in Porous Media Review and Evaluation with Special Emphasis on Capillary Liquid Transport*", Powder Technology, 11, 1975, p205-236
11. Dullien, F. A. L., "Porous Media: Fluid Transport and Pore Structure", Academic Press, Inc. New York, 1992, p1-574
12. Lohmander, S., Martinez, M., Lason, L., and Rigdahl, M., "*Dewatering of coating dispersions - model experiments and analysis*", Advanced Coating Fundamentals Symposium, Toronto, Tappi Press, Atlanta, 1999, p43-58

13. Levine, S., Reed, P., and Shutts, G., "*Some Aspects of Wetting/Dewetting of a Porous Medium*", Powder Technology, (17), 1977, p163-181
14. Seguin, D., Montillet, A., and Comiti, J., "*Experimental characterisation of flow regimes in various porous media - I: Limit of laminar flow regime*", Chemical Engineering Science, 53(21), 1998, p3751-3761
15. Seguin, D., Montillet, A., Comiti, J., and Huet, F., "*Experimental characterization of flow regimes in various porous media - II: Transition to turbulent regime*", Chemical Engineering Science, 53(22), 1998, p3897-3909
16. Schoelkopf, J., "*Observation and Modelling of Fluid Transport into Porous Paper Coating Structures*", PhD thesis, University of Plymouth, U.K., 2002
17. Schoelkopf, J., Gane, P. A. C., Ridgway, C. J., Spielmann, D. C., and Matthews, G. P., "*Rate of vehicle removal from offset inks: a gravimetric determination of the imbibition behaviour of pigmented coating structures*", Tappi 2001 Advanced Coating Fundamentals Symposium Proceedings, San Diego, Tappi, Atlanta, 2001, p1-18
18. Schoelkopf, J., Gane, P. A. C., and Ridgway, C. J., "*Observed non-linearity of Darcy permeability in compacted fine pigment structures*", Symposium: In Memory of Dr. Bernie Miller, TRI Princeton 2002
19. Spielmann, D. C., personal communication, 2002
20. German, Randall M., "Particle Packing Characteristics", Metal Powder Industries Federation, 1989, p1-443
21. Ridgway, C. J., Schoelkopf, J., Matthews, G. P., Gane, P. A. C., and James, P. W., "*The effects of void geometry and contact angle on the absorption of liquids into porous calcium carbonate structures*", Journal of Colloid and Interface Science, 239(2), 2001, p417-431
22. Ridgway, C. J., Schoelkopf, J., and Gane, P. A. C., "*A new method for measuring the liquid permeability of coated and uncoated papers and boards*", submitted to Journal of Pulp and Paper Science, 2002
23. Toivakka, M. and Nyfors, K., "*Pore space characterization of coating layers*", Tappi Journal, 84(3), 2001, p49-49
24. Gane, P. A. C., Ridgway, C. J., and Schoelkopf, J., "*Absorption Rate and Volume Dependency on the Complexity of Porous Network Structures*", submitted to Transport in Porous Media, 2002
25. Gane, P. A. C. and Seyler, E. N., "*Some aspects of ink/paper interaction in offset printing*", PTS Coating Symposium, Munich 1993
26. Gane, P. A. C., Seyler, E. N., and Swan, A., "*Some novel aspects of ink/paper interactions in offset printing*", International Printing and Graphic Arts Conference, Halifax, Nova Scotia, Tappi Press, Atlanta, 1994, p209-228